Low-frequency Variations of the Zonal Mean State of the Southern Hemisphere Troposphere

By Masato Shiotani

Department of Geophysics, Faculty of Science, Kyoto University, Kyoto 606, Japan
(Manuscript received 20 March 1990, in revised form 11 June 1990)

abstract

This paper presents an observational study of the low-frequency variation in the Southern Hemisphere troposphere, using the global analyses for 1980–85 provided by the European Center for Medium Range Weather Forecasts. An empirical orthogonal function (EOF) analysis is made for the zonal mean geopotential height at 1000 mb to capture the variation. Based on time series of the second EOF coefficients, which represent the dominant non-seasonal low-frequency variation in the Southern Hemisphere, we define four typical events: negative extreme (D−), positive extreme (D+), negative to positive transition (T+), and positive to negative transition (T−) events.

The variations on a hemispheric scale show a barotropic seesaw pattern with an almost axisymmetric node around 60°S and wavenumber 3 anomalies superimposed on it. Maximum westerlies at 500 mb are located at higher latitudes in D− event (50–60°S) than in D+ event (30–40°S). In association with the location of maximum westerlies, storm activity (defined as temporal variances of the high-pass (≤6 day) height field data) shows that large variation around 50°S occupies the entire latitude circle for a D− event but it is weaker in the western hemisphere for a D+ event.

Composite analyses on a daily basis are made of several physical quantities at 500 mb for the four events. It is found that the latitudinal movement of maximum westerlies is quicker in T+ events than in T− events, in addition to the higher-latitude maximum westerlies in D− events than in D+ events. The zonal mean temperature is colder at high latitudes and warmer at middle latitudes in D− events than in D+ events, corresponding to the stronger polar vortex resulting from the steeper temperature gradient and more vigorous storm activity in D− events than in D+ events.

The eddy momentum flux plays an important role especially during transition events; there is large equatorward transport of momentum at high latitudes around the key day of a T+ event and larger poleward transport at middle latitudes around the key day of a T− event. The heat flux seems to play a less important role. The acceleration of mean zonal winds is mainly determined as a residual between the momentum flux convergence and the Coriolis force.

1. Introduction

Since Wallace and Gutzler (1981) succeeded in describing teleconnection patterns in the Northern Hemisphere troposphere, a number of similar analyses have been carried out for the Southern Hemisphere. Using an empirical orthogonal function (EOF) analysis of mean sea level pressure (SLP) and 500 mb height anomalies based on daily synoptic maps, Rogers and van Loon (1982) showed that the principal component of the variation in the Southern Hemisphere is almost zonal with a nodal line around 60°S. Mo and White (1985) used the monthly mean dataset of SLP and 500 mb height anomalies to make an extensive analysis of the teleconnectivity in the Southern Hemisphere. In addition to an out-of-phase relation between high and middle latitudes similar to that reported by Rogers and van Loon, they found a striking wavenumber 3 pattern over the southern ocean.

Because this variation is basically zonal and barotropic, several researchers investigating zonal mean quantities have looked at different aspects of the variation in the Southern Hemisphere. Trenberth and Christy (1985) described the low-frequency variation in the monthly mean dataset of the zonal mean SLP which represents the zonal mass distribution of the atmosphere. Although their analysis included the Northern and Southern hemispheres, the principal component of their EOF analysis is a dipole mode restricted to the Southern Hemisphere with a nodal latitude around 60°S. Recently, Christy *et al.* (1989) have made a detailed analysis of surface pressure variations using daily but filtered (30–75 day) data. They confirmed that

the leading modes are essentially similar to those described by Trenberth and Christy (1985) who used monthly mean data.

The zonal mean wind field in the Southern Hemisphere also shows a similar low-frequency variation. Yoden *et al.* (1987) found two typical regimes of the mean zonal geostrophic winds during the winter of 1983: a single-jet regime, and a double-jet regime. In the single-jet regime the subtropical jet at the tropopause level is strong, but in the double-jet regime the subtropical jet is weak and the polar night jet extends down to the surface at about 55°S. The principal component of their EOF analysis for the zonal mean winds in a latitude-height plane shows a barotropic dipole pattern with a nodal latitude around 45°S. Kidson (1988a) has shown a similar variation in the zonal mean wind field at 500 mb based on a 15-year dataset.

Moreover, relations of the low-frequency variation with wave quantities such as eddy momentum flux and eddy heat flux have been investigated by Kidson (1988b) who used a twice-daily but filtered dataset in which a mean annual cycle and variations with periods less than 50 days were removed. Though he found some interesting features between the low-frequency variation in the height field and wave quantities, these results were only presented by calculating correlations.

The purpose of this study is to investigate the low-frequency variation in the Southern Hemisphere troposphere using unfiltered daily data, while almost all previous studies on this subject were based on monthly mean or daily but filtered data. With the use of daily data, attention can be focused on the life cycle of the low-frequency variation.

After describing the data used in this study in Section 2, we make an EOF analysis for the mean zonal geopotential height field at 1000 mb to calculate an index of the low-frequency variation, and then define four typical events (two extreme events and two transition events). Some aspects of the variation are compared with previous works (Section 3). In Section 4 a key day analysis is made for the four events. A summary and discussion are found in Section 5.

2. Data

The global analyses of temperature, geopotential height, and wind speed (u- and v-components) derived by the European Center for Medium Range Weather Forecasts (ECMWF) is used for the 6 years from 1980 to 1985. The ECMWF data were reduced from the original twice-daily 2.5° × 2.5° longitude-latitude grids into daily 5° × 5° longitude-latitude grids. We preferred to use 0000 UTC rather than 1200 UTC analyses because, as Trenberth (1979) notes, the coverage of original station data in the Southern Hemisphere is generally better at the former time. Wave statistics were then calculated for

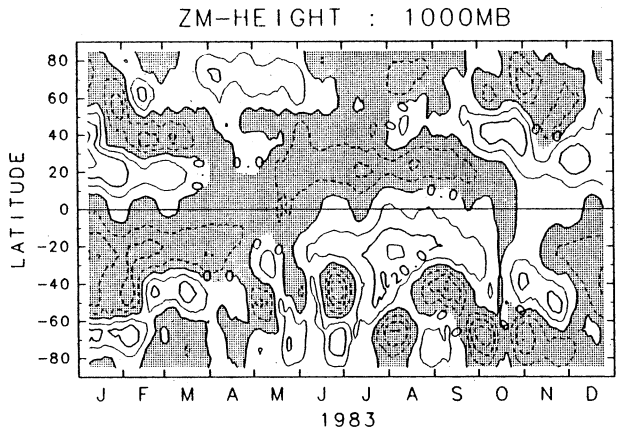

Fig. 1. Time-latitude section of the area weighted zonal mean geopotential height $[Z_s]$ (contour interval 10 m) at 1000 mb in 1983. Time mean for each latitude is subtracted. Negative values are shaded.

zonal wavenumbers 1 through 12. Because the low-frequency variation is basically barotropic, analyses are concentrated on the 500 mb level; however, the zonal mean height at 1000 mb is used to define an index of the variation.

3. EOF analysis for 1000 mb [Z]

Figure 1 shows a time-latitude section of the area-weighted zonal mean geopotential height at 1000 mb, $[Z_{1000}]\cos\phi$ with the time mean for each latitude subtracted and a 15-day running mean applied to remove synoptic scale variability. Hereafter, we refer to $[Z_{1000}]\cos\phi$ as $[Z_s]$. The height field at 1000 mb can be assumed to be representative of the sea level pressure and thus the atmospheric mass distribution. At low latitudes there is a clear annual variation which is antisymmetric with respect to the equator. On the other hand at middle and high latitudes, there are dipole variations with a nodal latitude around 60°, especially during winter and spring in the Southern Hemisphere. Its characteristic time scale is about 1 to 2 months.

We selected the year of 1983 as an example to examine the relation of $[Z_s]$ to the low-frequency variation in the zonal mean wind field reported by Yoden *et al.* (1987). Four typical periods they defined in terms of the latitudinal structure of the zonal winds from mid-June through mid-October are clear in Fig. 1 (refer to Fig. 1 in Yoden *et al.*); when $[Z_s]$ at high latitudes was relatively high they observed only one latitudinal maximum of the zonal mean westerlies at subtropical latitudes in the upper troposphere, but when it was relatively low they observed another maximum at high latitudes. The relation to the wind field is reasonable because the dipole variation about 60°S has a barotropic structure. Indeed a coherent variation in $[Z]$ can be seen in the whole troposphere, though the annual component is larger

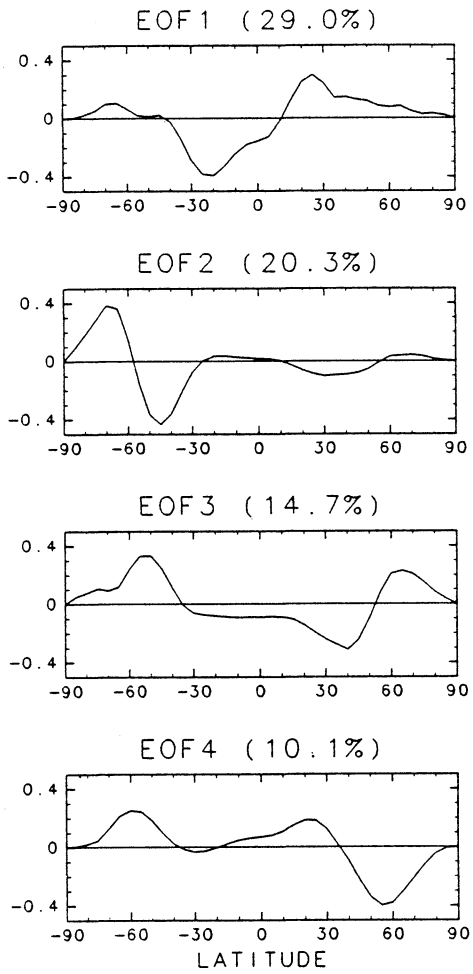

Fig. 2. The first four EOF profiles of $[Z_s]$. Contribution to the total variance is written in parentheses.

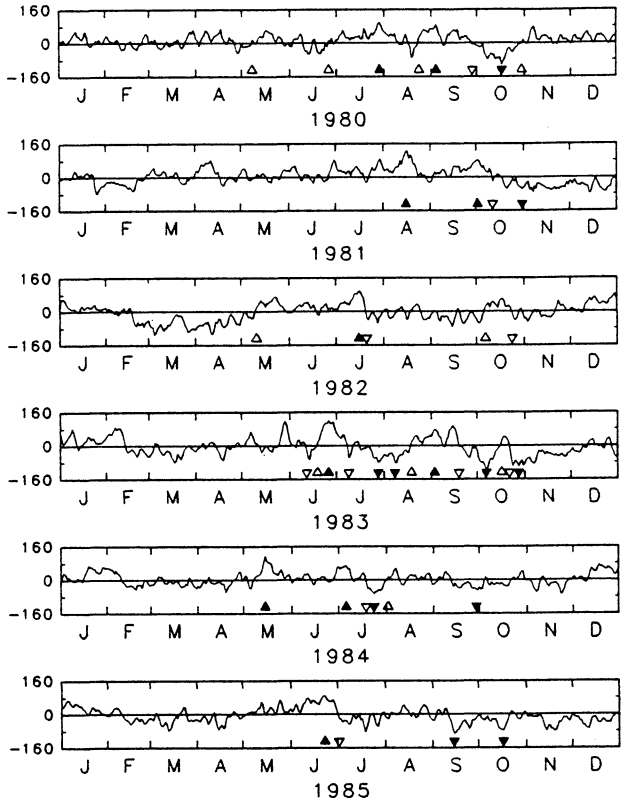

Fig. 3. Time series of the second EOF amplitudes (unit m). Key days for D−, T+, D+ and T− events are shown as marks of ▼, △, ▲ and ▽, respectively.

in the upper than in the lower troposphere. Similar variations in the zonal mean sea level pressure were first reported by Trenberth and Christy (1985) and detailed by Christy *et al.* (1989). Their latitudinal modes of the variation will be compared with our results below.

To define an index of the low-frequency variation and to confirm that the dipole mode in the Southern Hemisphere is really an intra-hemispheric mode, we made an EOF analysis on the basis of the cross-covariance matrix of the daily zonal mean height field at 1000 mb $[Z_s]$ for both hemispheres. (In preliminary analyses, we found that filtering such as removing high frequency or annual components is not essential to extract the characteristic variations in the Southern Hemisphere.)

Figure 2 shows the first four dominant components, each of which contributes over 10% to the total variance. EOF 1 represents the seasonal cycle at low latitudes. EOF 2 is a dipole mode largely restricted to the Southern Hemisphere. EOFs 3 and 4 are global symmetric and antisymmetric modes with respect to the equator, respectively. Such global modes (EOFs 3 and 4) might be related to normal modes of the shallow water equations for zonal wavenumber zero (Shigehisa, 1983). Although our analysis is based on the daily, unfiltered dataset, the modes in Fig. 2 (except the annual cycle mode, EOF 1) are almost identical to those calculated by Christy *et al.* (1989) who used daily but band-pass (30–75 day) filtered data for zonal mean surface pressure. This means that the variations represented by EOFs 2, 3, and 4 in this study are basically low-frequency in nature and that most of the variance in $[Z_s]$ can be explained by the low-frequency variability of the atmosphere. Hereafter, we will concentrate on time series of the EOF 2 amplitudes (Fig. 3); they were calculated in such a way that the daily values of $[Z_s]$ are multiplied by the EOF profile. Though there is a small contribution from the Northern Hemisphere to EOF 2, time series of the EOF 2 amplitudes do not change much even if the contribution in the Northern Hemisphere is set to zero.

On the basis of this time series (Fig. 3), we define four typical events and select 10 cases for each of the four events. The selection was limited to the period from May to October where the seasonal variation of $[Z_s]$ is small (Fig. 1). First we define two extreme states: when the EOF 2 amplitudes are larger than

Table 1. Key days for each of the four events.

D− event			T+ event			D+ event			T− event		
16	Oct	1980	7	May	1980	28	Jul	1980	27	Sep	1980
30	Oct	1981	25	Jun	1980	3	Sep	1980	11	Oct	1981
27	Jul	1983	23	Aug	1980	15	Aug	1981	20	Jul	1982
7	Aug	1983	29	Oct	1980	1	Oct	1981	23	Oct	1982
6	Oct	1983	10	May	1982	15	Jul	1982	11	Jun	1983
27	Oct	1983	6	Oct	1982	25	Jun	1983	8	Jul	1983
23	Jul	1984	18	Jun	1983	2	Sep	1983	18	Sep	1983
28	Sep	1984	18	Aug	1983	14	May	1984	21	Oct	1983
14	Sep	1985	16	Oct	1983	5	Jul	1984	18	Jul	1984
16	Oct	1985	1	Aug	1984	22	Jun	1985	1	Jul	1985

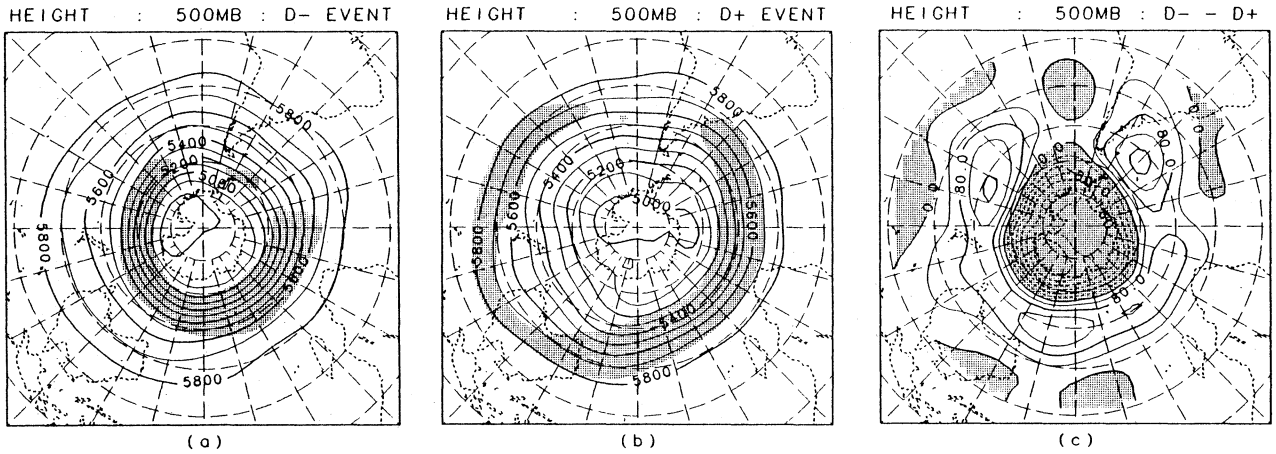

Fig. 4. Synoptic charts projected on a stereographic grid (poleward from 15°S is shown) of the geopotential height field made from 10 case composite for (a) D− events, (b) D+ events (contour interval 100 m) and (c) difference between D− and D+ events (contour interval 40 m). Regions over 20 ms^{-1} of the u-wind are shaded in (a) and (b). Negative values are shaded in (c).

$+1\sigma$ (σ : standard deviation of the time series) with a duration over 7 days we call it a D+ event, and when they are smaller than -1σ with a duration over 8 days we call it a D− event. Key days are defined when the EOF 2 amplitude is greatest in a D+ event and least in a D− event. From the definition of the EOF 2 profile, a D+ event corresponds to high values of the zonal mean height field at high latitudes and low values at middle latitudes. These departures are reversed in a D− event. Next we define two transition events: when the time series of EOF 2 changes from below -1σ to more than $+1\sigma$ within 17 days, we call it a T+ event and the first day with a positive value is the key day. The opposite transition is called a T− event. We adjusted the threshold of the duration to select the same number of cases for the four events. Table 1 lists the key days of each of 10 cases of the four events. Selected cases are independent and not necessarily consecutive. Their number differs from year to year in agreement with Yoden *et al*'s (1987) finding that the low-frequency variation in the zonal winds is not clear in every year. This suggests that there exists the interannual variability of the low-frequency variation.

To compare the hemispheric anomaly patterns characterized by D− and D+ events with those observed by previous studies, composite synoptic maps of the geopotential height field at 500 mb for D− and D+ events are shown in Fig. 4a and 4b, respectively; regions where u-wind speed exceeds 20 ms^{-1} are hatched. These composites are the mean of 10 events in which a 7-day average is taken about the key day. Both of the two maps show almost circular isopleths. However, because of the lower pressure at polar latitudes in D− events, isopleths are denser at high latitudes resulting in stronger westerlies there in D− events. On the other hand in a D+ event, a westerly jet is located at middle latitudes. Moreover, isopleths in D+ events are distorted with a zonal wavenumber 3 pattern. This suggests that a D+ events is related to the wave 3 type of blocking episodes which are frequently observed in the Southern Hemisphere (Trenberth and Mo, 1985; Mo, 1986; Hansen and Sutera, 1988).

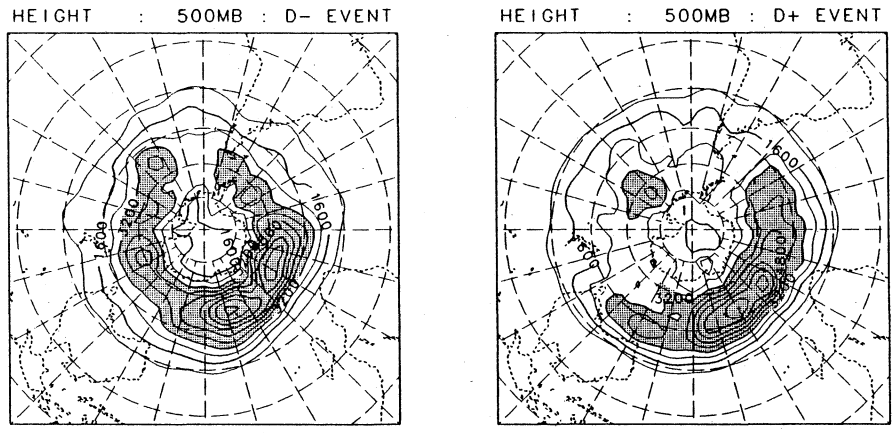

Fig. 5. As in Fig. 4 but for the variance of the high-pass filtered geopotential height (contour interval 800 m^2). Regions over 3200 m^2 are shaded.

The difference between the two (D− event minus D+ event) can characterize this low-frequency variation (Fig. 4c). The variation is on a hemispheric scale with an almost circular node around 60°S, but zonal wavenumber 3 anomalies over the southern ocean are superimposed on it. These features are essentially similar to those of the principal EOF pattern depicted from hemispheric analyses of the Southern Hemisphere (cf. Rogers and van Loon, 1982; Mo and White, 1985; Mo and Ghil, 1987; Kidson, 1988b).

In association with the location of the westerly jet, storm activity is briefly examined on the basis of high-pass (≤6 day) filtered data; we use the high-pass filtered data to focus on the time scale of baroclinic disturbances and to describe the so-called storm track (cf. Wallace and Blackmon, 1983). Figure 5 shows the geographical distribution of the event-mean temporal variance calculated for 15 days of the high-pass 500 mb height field for D− and D+ events. We have checked that the results are not sensitive to the length of events for calculating temporal variance. As Trenberth (1981) showed based on eight years of data, high-frequency fluctuations are maximum in the southern Indian Ocean. In the South Pacific sector, however, there is a clear difference between D− and D+ events. In a D− event, corresponding to the stronger westerlies at higher latitudes, the storm track defined by large variances is located around the Antarctic continent. In a D+ event, the large variance zone around the South Pacific is not clear and seems to shift toward low latitudes in the south of Australia. This shift or block of the storm track might be due to blocking events in the New Zealand sector where blocking events in the Southern Hemisphere prefer to occur (Trenberth and Mo, 1983; Lejenäs, 1984).

4. Life cycle analysis

In this section, sequences of the four events on a daily basis are investigated by presenting composite time-latitude sections; day 0 is the key day of each of the four events. To simplify the plots a 5-day running mean was applied for Figs. 6–11. From the definition of the four events, it is meaningless to say anything about the time interval between successive events; in other words, periodicity cannot be assumed for the low-frequency variation in this study. The sequence runs in the following order: D−, T+, D+ and T− event. Although time scales of the four events would be different, sampling number is too small to evaluate each of them. The longest interval of successive events in Table 1 is 34 days, the shortest one is 5 days, and the average is 14 days. Thus we will focus our attention on about 2 weeks around the key day in the following figures.

The first sequence is for the mean zonal wind at 500 mb (Fig. 6). As we saw in Fig. 4, extreme events are characterized by maximum westerlies at higher latitudes in a D− event than in a D+ event. The location of maximum westerlies is stable in a D− event, but it moves poleward much faster after the key day of a D+ event. In connection with this movement, the transition is faster in a T+ event than in a T− event; in a T+ event the westerly jet moves about 10° toward the equator in a few days, but in a T− event it moves gradually.

Figure 7 shows a composite sequence for the zonal mean temperature. In these figures, the time mean of the whole period is subtracted at each latitude. Around the key day of the extreme events, the zonal mean temperature at high latitudes is colder in D− events than in D+ events; at middle latitudes, it is warmer in D− events than in D+ events. This means a steeper temperature gradient, resulting stronger westerlies at high latitudes, in a D− event than in a D+ event. In the transition periods, features are not clear but there are opposing changes of the temperature tendency at high and middle latitudes.

Interesting sequences are presented in Fig. 8 for the eddy momentum flux $[u^*v^*]$. In a D− event,

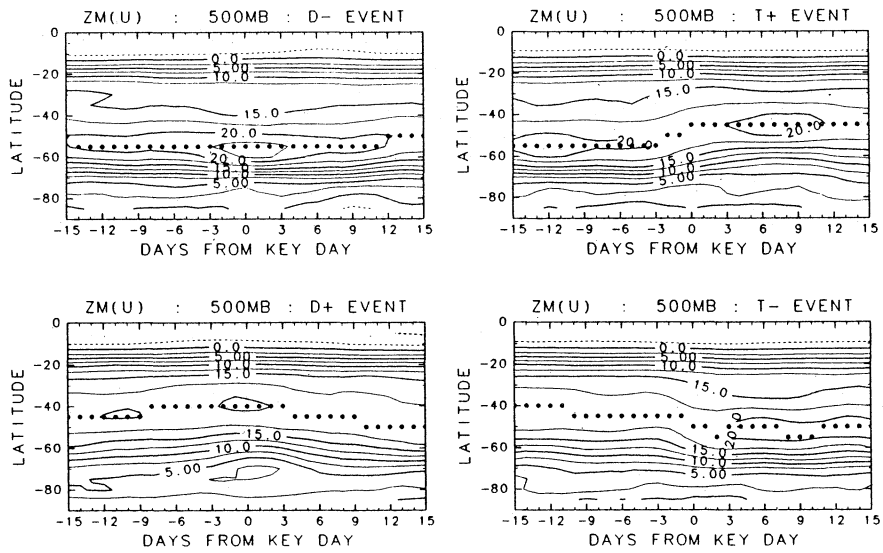

Fig. 6. Composite time-latitude sections of the mean zonal wind (contour interval 2.5 ms^{-1}) at 500 mb for the four events. Latitudinal maxima are dotted.

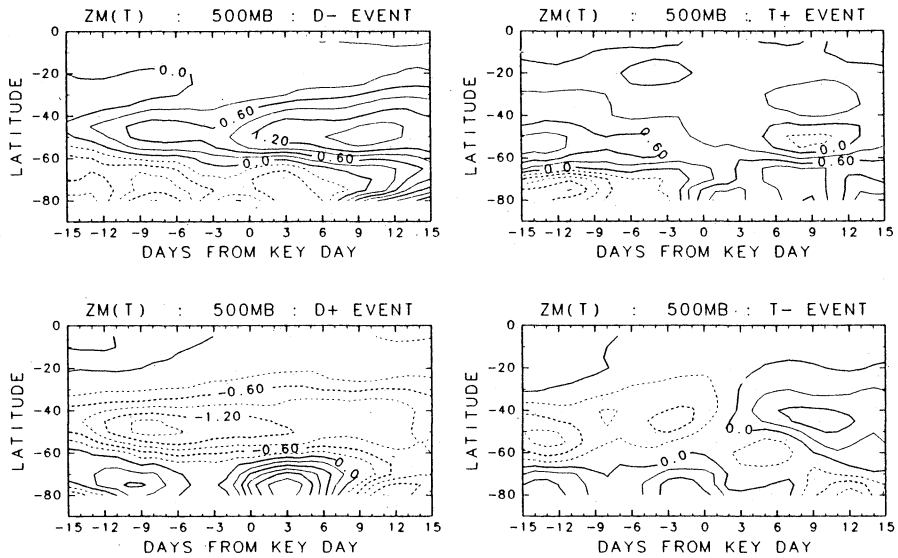

Fig. 7. As in Fig. 6 but for the zonal mean temperature (contour interval 0.3K). The mean for the whole period for each latitude is subtracted.

there is stronger poleward transport around 40°S; its extreme value appears a few days before the key day and its magnitude decreases around the key day. In a T+ event, just on the key day, equatorward transport at high latitudes around 65°S is maximum and poleward transport at middle latitudes is weak. This equatorward transport at high latitudes continues during the latter half of a T+ event and the first half of a D+ event. Around the key day of a D+ event, the equatorward transport at high latitudes is suddenly weakened, and the poleward transport at middle latitudes is strengthened. In a T− event, strong poleward transport appears around the key day. The effect of the momentum flux convergence on accelerating the zonal wind will be discussed in Figs. 10 and 11.

Kidson (1988b) calculated correlations between time series of the momentum flux and an index defined by his EOF analysis which describes the low-frequency variation in the Southern Hemisphere; the variation he found is essentially similar to that of our study. He obtained a maximum correlation where changes in the momentum flux lead the index by 4.5–5 days. Our results of the sequence for the eddy momentum flux support his statistics and suggest an important role for transient eddies particularly during the transition periods.

As for the eddy heat flux $[v^*T^*]$, Yoden *et al.* (1987) showed that it has larger negative values around the mid-latitude troposphere in the single-

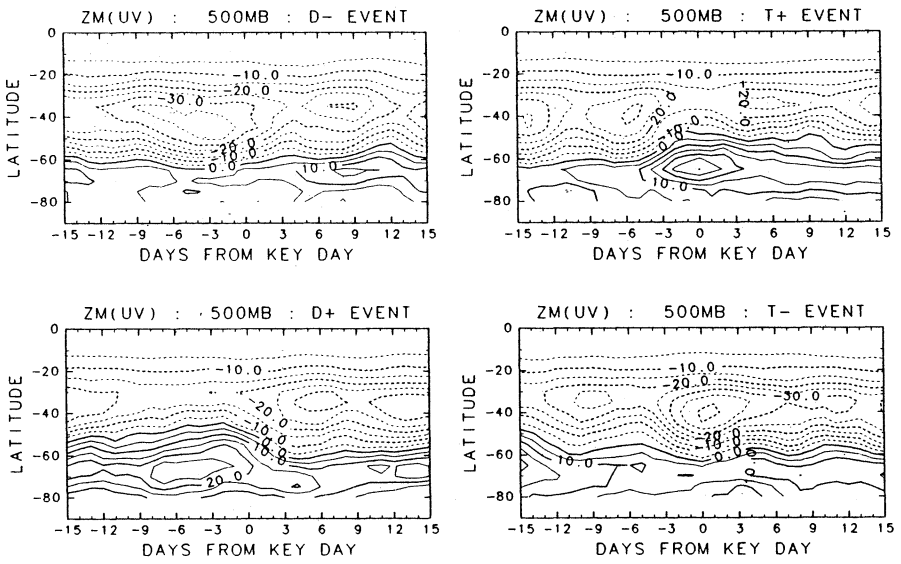

Fig. 8. As in Fig. 6 but for the eddy momentum flux (contour interval 5 $m^2 s^{-2}$).

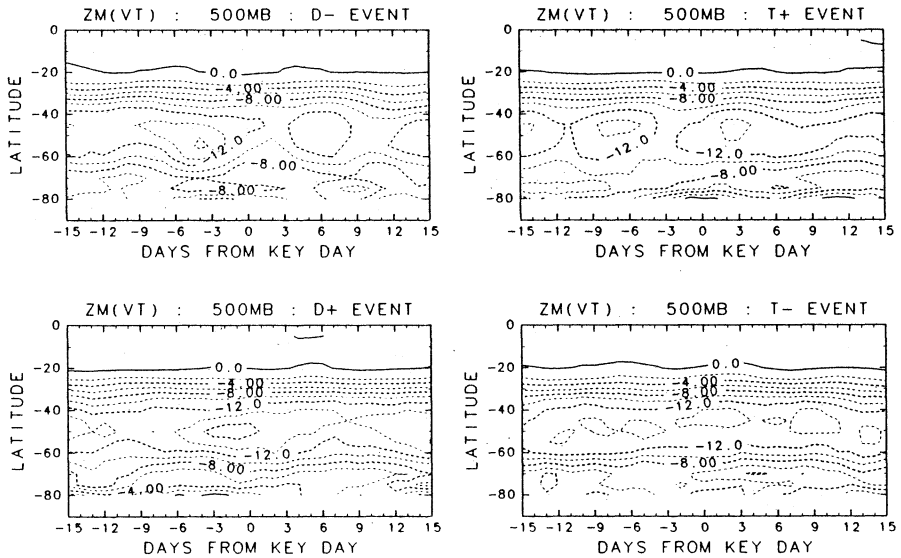

Fig. 9. As in Fig. 6 but for the eddy heat flux (contour interval 2 $ms^{-1}K$).

jet regime (corresponding to a D+ event) than in the double-jet regime (corresponding to a D− event). In our composite analysis for the heat flux (Fig. 9), however, differences among the four events are not clear. In fact, there are slightly larger negative values in D+ events than in D− events, as Yoden *et al.* (1987) showed, but they are not so significant as the result of the eddy momentum flux. Kidson (1988b) also showed smaller correlation coefficients for the heat flux than for the momentum flux.

Finally we investigate the acceleration in the mean zonal wind ($\partial[u]/\partial t$) and the balance between the eddy momentum flux convergence $-(a\cos^2\phi)^{-1}\partial([u^*v^*]\cos^2\phi)/\partial\phi$ and Coriolis torque $f[v]$. (Hereafter we refer to $-(a\cos^2\phi)^{-1}\partial([u^*v^*]\cos^2\phi)/\partial\phi$ as $-[u^*v^*]_\phi$.) Figure 10 shows a composite sequence of the zonal acceleration for the four events at 500 mb. As deduced from Fig. 6, dipole patterns of acceleration and deceleration at high and middle latitudes are clear around the key day of T+ and T− events. In D− and D+ events, two pairs of the dipole pattern are observed a few days before and after the key day. The momentum balances are next investigated at two latitude bands, 60°S and 40°S, where the variation of the zonal acceleration is distinctive. Figure 11 shows the result at 60°S and 500 mb; the result for 40°S is essentially similar. To estimate the momentum balance more exactly it is necessary to calculate the vertical convergence of the vertical momentum flux and an unknown drag term probably due to gravity waves. In this study, however, only the eddy momentum flux convergence $-[u^*v^*]_\phi$, Coriolis torque $f[v]$, and $\partial[u]/\partial t$ (denoted as DM, FV and DU in Fig. 11) are estimated. First

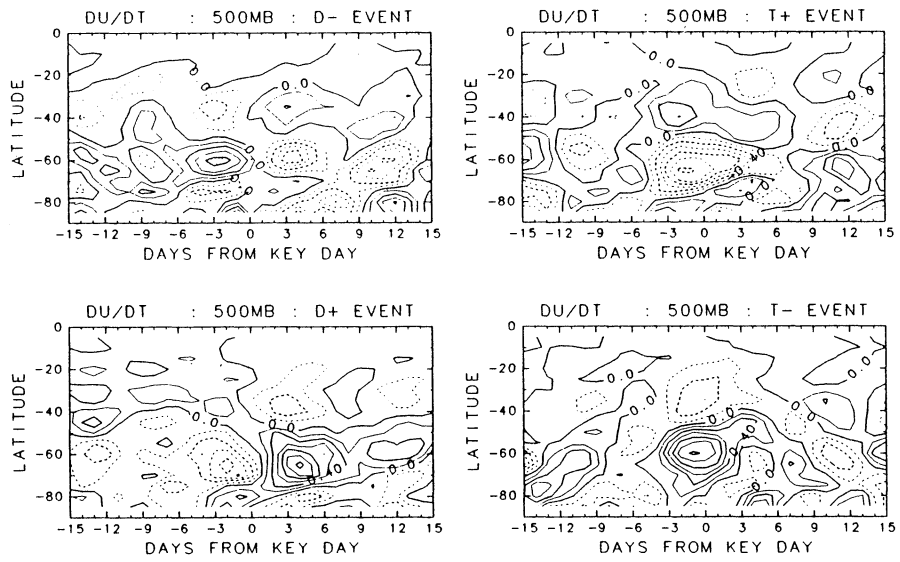

Fig. 10. As in Fig. 6 but for $\partial[u]/\partial t$ (contour interval 0.2 $ms^{-1}day^{-1}$).

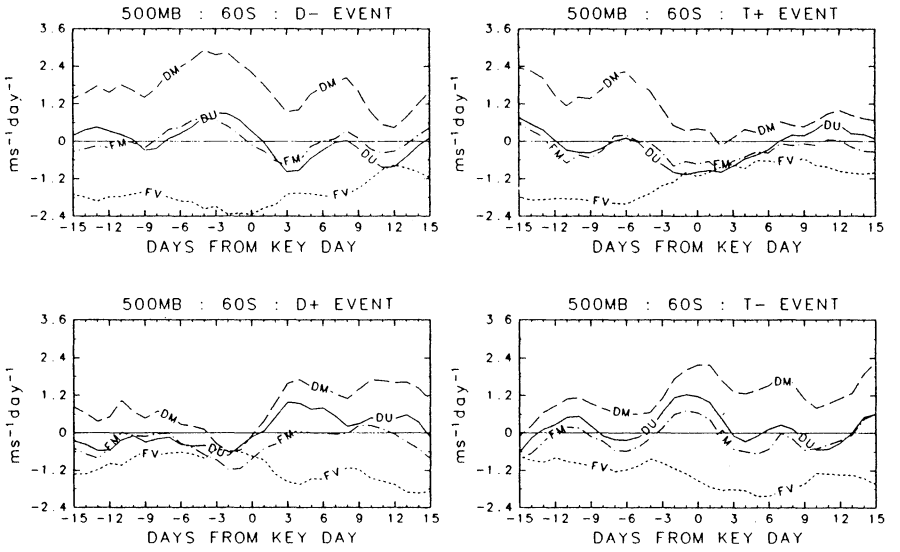

Fig. 11. Line plots of the eddy momentum flux convergence (DM), Coriolis torque (FV), sum of the two (FM=DM+FV), and $\partial[u]/\partial t$ (DU). Units are $ms^{-1}day^{-1}$.

of all, it is clear that an imbalance between $-[u^*v^*]_\phi$ and $f[v]$ (denoted as FM in Fig. 11) reasonably explains the zonal acceleration $\partial[u]/\partial t$. In general, this imbalance is a small residual between large values of $-[u^*v^*]_\phi$ and $f[v]$. The two terms of $-[u^*v^*]_\phi$ and $f[v]$ vary consistently, but the tendency in $\partial[u]/\partial t$ is mainly determined by that of $-[u^*v^*]_\phi$. These results mean that time changes in the zonal mean westerlies for each of the four events are due to the barotropic conversion associated with transient eddy momentum fluxes and accompanying changes of Coriolis torque, though it does not imply any causal relationships merely that the system remains balanced.

5. Conclusions

We have investigated low-frequency variations in the Southern Hemisphere, using unfiltered daily datasets for 6 years provided by the ECMWF. The EOF analysis of the zonal mean geopotential height at 1000 mb has shown that the second dominant profile is a dipole mode restricted to the Southern Hemisphere; this mode explains 20.3 % of the total variance, though the original dataset includes the annual component. Variations on a hemispheric scale show a barotropic seesaw pattern with an almost circular node around 60°S. The dominant mode of low-frequency variations in the Northern Hemisphere shows a similar north-south seesaw pattern, though the mode in the Northern Hemisphere does not have such a clear circular node as in the Southern Hemisphere (cf. Trenberth and Paolino, 1981; Rogers, 1981). By analyzing a 15-year GCM simulation with fixed external forcing, Lau (1981) showed that vari-

ations in the Northern Hemisphere are dominated by a similar north-south seesaw pattern. Thus we may regard the low-frequency seesaw variation as a natural mode of the atmosphere.

Based on time series of the dominant EOF coefficients in the Southern Hemisphere, we have defined four typical events: two extreme events (D− and D+) and two transition events (T+ and T−). The variation is closely related to the wind field; there are stronger westerlies at high latitudes in a D− event and at middle latitudes in a D+ event. Although these variations are basically zonal, a planetary wavenumber 3 is dominant in D+ events. Because Trenberth and Mo (1985) and Mo (1986) showed that blocking episodes of the wave 3 type are frequently observed in the Southern Hemisphere, D+ events seem to be related to such blocking events. Moreover, temporal variances of the high-pass (≤ 6 day) height field data, which represent synoptic-scale wave activity, show that large variations around 50°S are confined in the eastern hemisphere for D+ events but they exist around the whole latitude circle for D− events. The active region in the western hemisphere corresponds to maximum westerlies at high latitudes for D− events. The different storm activity in the South Pacific sector between the two events might be related to the double maximum distribution of cyclone centers in this region (Taljaard, 1972).

Further attention has been paid to the two transition periods (T+ and T− events) by making key-day composite analyses for several physical quantities. In time-latitude sections of the mean zonal winds, it was found that the transition in a T+ event is generally faster than in a T− event. In the sequence of zonal mean temperatures, it is colder at high latitudes in D− events than in D+ events. This means steeper temperature gradients, resulting in vigorous storm activity and stronger westerlies at high latitudes, in D− events than in D+ events.

The most remarkable signals during the transition events can be seen in the eddy momentum flux. There are larger equatorward transports of momentum at high latitudes around the key day of T+ events and larger poleward transports at middle latitudes around the key day of T− events. The sense of momentum flux is relevant to the latitudinal movement of maximum westerlies. There also exist signals in the momentum flux a few days before the key day of D− and D+ events. These results suggest that barotropic conversions involving the transient eddy momentum flux are important for the transition between and attainment of extreme events. It is found on a daily basis that the acceleration of the mean zonal wind is reasonably represented as a residual between the eddy momentum flux convergence and Coriolis torque. The two terms have large values compared with the acceleration term, but cancel out leaving a small imbalance to produce the zonal acceleration. Although Newell *et al.* (1972) and Trenberth (1987) found similar results for the seasonal-mean momentum budget, our results have shown that it is also the case on a daily basis.

The dominant variation in the Southern Hemisphere has a characteristic timescale of one to two months; this time scale is close to that of the so-called 30–60 day variation in the equatorial region. In fact, the variation in the tropical geopotential height field has a zonal structure with little phase differences (Nishi, 1989). Moreover, Risbey and Stone (1988) showed a possible link between equatorial and Southern Hemisphere extratropical latitudes involving the zonal mean momentum for the frequency band of 30–60 day. As we saw in EOF 2 (Fig. 2), however, the mode has little contribution from equatorial latitudes. In preliminary analyses, we calculated correlation coefficients between time series of EOF 2 and outgoing long-wave radiation data, but could not find any significant values in the equatorial region. Recently, Nishi (personal communication) investigated the interannual variability of the 30–60 day variation using rawinsonde data of 6 stations located between 5–10°N and 130–175°E from 1979 to 1987. He finds that during Southern Hemisphere winters of 1980 and 1983 the variation is small, but these are when the low-frequency variation we focused on in this study is dominant (Fig. 3 or Table 1). Therefore we conclude that the low-frequency variation in the Southern Hemisphere is not directly related to the 30–60 day variation in the equatorial latitudes, although it tends to be diminished when the 30–60 day variation is active.

Our composite key-day analyses were only performed for zonal quantities, because we found that wave quantities such as the eddy momentum and heat fluxes for each case of the four events do not seem to reproduce similar features on synoptic maps, although they are reproducible in a zonal mean sense. As a step beyond the present study, we should accumulate case studies like Trenberth (1986) to develop a three-dimensional view of the wave action on the background flow for each stage of the low-frequency variation.

Acknowledgment

I wish to thank Shigeo Yoden and Noriyuki Nishi for stimulating discussions. The computations were performed at the Data Processing Center of Kyoto University. The NCAR graphic package was used for some graphic outputs.

References

Christy, J.R., Trenberth, K.E. and Anderson, J.R., 1989: Large-scale redistributions of atmospheric mass. *J. Climate*, **2**, 137–148.

Hansen, A.R. and Sutera, A., 1988: Planetary wave amplitude bimodality in the southern hemisphere. *J. Atmos. Sci.*, **45**, 3771–3783.

Kidson, J.W., 1988a: Indices of the southern hemisphere zonal wind. *J. Climate*, **1**, 183–194.

Kidson, J.W., 1988b: Interannual variations in the southern hemisphere circulation. *J. Climate*, **1**, 1177–1198.

Lau, N.-C., 1981: A diagnostic study of recurrent meteorological anomalies appearing in a 15-year simulation with a GFDL general circulation model. *Mon. Wea. Rev.*, **109**, 2287–2311.

Lejenäs, H., 1984: Characteristics of southern hemisphere blocking as determined from a time series of observational data. *Quart. J. Roy. Meteor. Soc.*, **110**, 967–979.

Mo, K.C., 1986: Quasi-stationary states in the southern hemisphere. *Mon. Wea. Rev.*, **114**, 808–823.

Mo, K.C. and White, G.H., 1985: Teleconnections in the southern hemisphere. *Mon. Wea. Rev.*, **113**, 22–37.

Mo, K.C. and Ghil, M., 1987: Statistics and dynamics of persistent anomalies. *J. Atmos. Sci.*, **44**, 877–901.

Newell, R.E., Kidson, J.W., Vincent, D.G. and Boer, G.J., 1972: *The general circulation of the tropics and interactions with extratropical latitudes*, Vol. 1. MIT Press, 258 pp.

Nishi, N., 1989: Observational study on the 30–60 day variations in the geopotential and temperature fields in the equatorial region. *J. Meteor. Soc. Japan*, **67**, 187–203.

Risbey, J.S. and Stone, P.H., 1988: Observations of the 30–60 day oscillation in zonal mean atmospheric angular momentum and high cloud cover. *J. Atmos. Sci.*, **45**, 2026–2038.

Rogers, J.C., 1981: Spatial variability of seasonal sea level pressure and 500 mb height anomalies. *Mon. Wea. Rev.*, **109**, 2093–2106.

Rogers, J.C. and van Loon, H., 1982: Spatial variability of sea level pressure and 500 mb height anomalies over the southern hemisphere. *Mon. Wea. Rev.*, **110**, 1375–1392.

Shigehisa, Y., 1983: Normal modes of the shallow water equations for zonal wavenumber zero. *J. Meteor. Soc. Japan*, **61**, 479–494.

Taljaard, J.J., 1972: Synoptic meteorology of the southern hemisphere. *Meteor. Monogr.*, **13–35**, 139–213.

Trenberth, K.E., 1979: Interannual variability of the 500 mb zonal mean flow in the southern hemisphere. *Mon. Wea. Rev.*, **107**, 1515–1524.

Trenberth, K.E., 1981: Observed southern hemisphere eddy statistics at 500 mb: frequency and spatial dependence. *J. Atmos. Sci.*, **38**, 2585–2605.

Trenberth, K.E., 1986: An assessment of the impact of transient eddies on the zonal flow during a blocking episode using localized Eliassen-Palm flux Diagnostics. *J. Atmos. Sci.*, **43**, 2070–2087.

Trenberth, K.E., 1987: The role of eddies in maintaining the westerlies in the southern hemisphere winter. *J. Atmos. Sci.*, **44**, 1498–1508.

Trenberth, K.E. and Paolino, Jr., D.A., 1981: Characteristic patterns of variability of sea level pressure in the northern hemisphere. *Mon. Wea. Rev.*, **109**, 1169–1189.

Trenberth, K.E. and Christy, J.R., 1985: Global fluctuations in the distribution of atmospheric mass. *J. Geophys. Res.*, **90**, 8042–8052.

Trenberth, K.E. and Mo, K.C., 1985: Blocking in the southern hemisphere. *Mon. Wea. Rev.*, **113**, 3–21.

Wallace, J.M. and Gutzler, D.S., 1981: Teleconnections in the geopotential height field during the northern hemisphere winter. *Mon. Wea. Rev.*, **109**, 784–812.

Wallace, J.M. and Blackmon, M.L., 1983: Observations of low-frequency atmospheric variability. *Large-scale dynamical processes in the atmosphere.* Eds, Hoskins, B.J. and Pearce, R.P., Academic Press, 55–94.

Yoden, S., Shiotani, M. and Hirota, I., 1987: Multiple planetary flow regimes in the southern hemisphere. *J. Meteor. Soc. Japan*, **65**, 571–586.

南半球対流圏における帯状平均場の長周期変動について

塩谷雅人

(京都大学理学部)

ヨーロッパ中期気候予報センターが提供する1980年から1985年までの全球解析データを用いて、南半球対流圏における長周期変動に関する観測的研究をおこなった。まず、1000 mbの帯状平均高度場のデータに対して経験的直交関数(EOF)解析をおこないこの変動をとらえた。EOF解析の第2成分（この成分が南半球において卓越する、季節変動成分とは異なる長周期変動を代表する）の時系列にもとづいて以下の4つの典型的なイベントを定義した：負極のイベント(D−)、正極のイベント(D+)、負から正への遷移イベント(T+)、正から負への遷移イベント(T−)。

半球規模のこの変動は、60°S付近にほぼ軸対称的な節を持ち波数3の偏差がその上に重なった順圧的なシーソーパターンを示す。500 mbにおける西風の最大はD+イベント(30–40°S)よりD−イベント(50–

60°S) のほうが高緯度に位置する。西風最大の位置と関連して傾圧波動の活動性（ハイパス (≤ 6 日) フィルターをかけた高度場の時間変動として定義する）は、D−イベントでは 50°S 付近の緯度円をぐるりととり囲むようにしてその活発域が存在するのに対し、D+イベントでは東半球に限られる。

次に、4 つのイベントについて 500 mb におけるいくつかの物理量に関しコンポジット解析をおこなった。西風の最大が D+イベントにより D−イベントのほうが高緯度に位置するのに加えて、その時間的な緯度方向の動きは T−イベントより T+イベントの方が速い。帯状平均した温度については、D+イベントより D−イベントの方が高緯度で冷たく中緯度で暖かい。これは D+イベントより D−イベントにおいて温度勾配が急で傾圧波動の活動性が活発なために極夜ジェットが強いことと対応している。

渦運動量輸送は特に遷移イベントにおいて重要な役割を果たす。T+イベントの基準日付近では、高緯度において赤道向きの大きな運動量輸送が見られる。いっぽう T−イベントの基準日付近では、中緯度において極向きの大きな運動量輸送が見られる。これに対し、熱輸送は重要な役割を果していない。また平均帯状風の加速はおもに運動量輸送の収束とコリオリの力との残差として決まっていることがわかった。